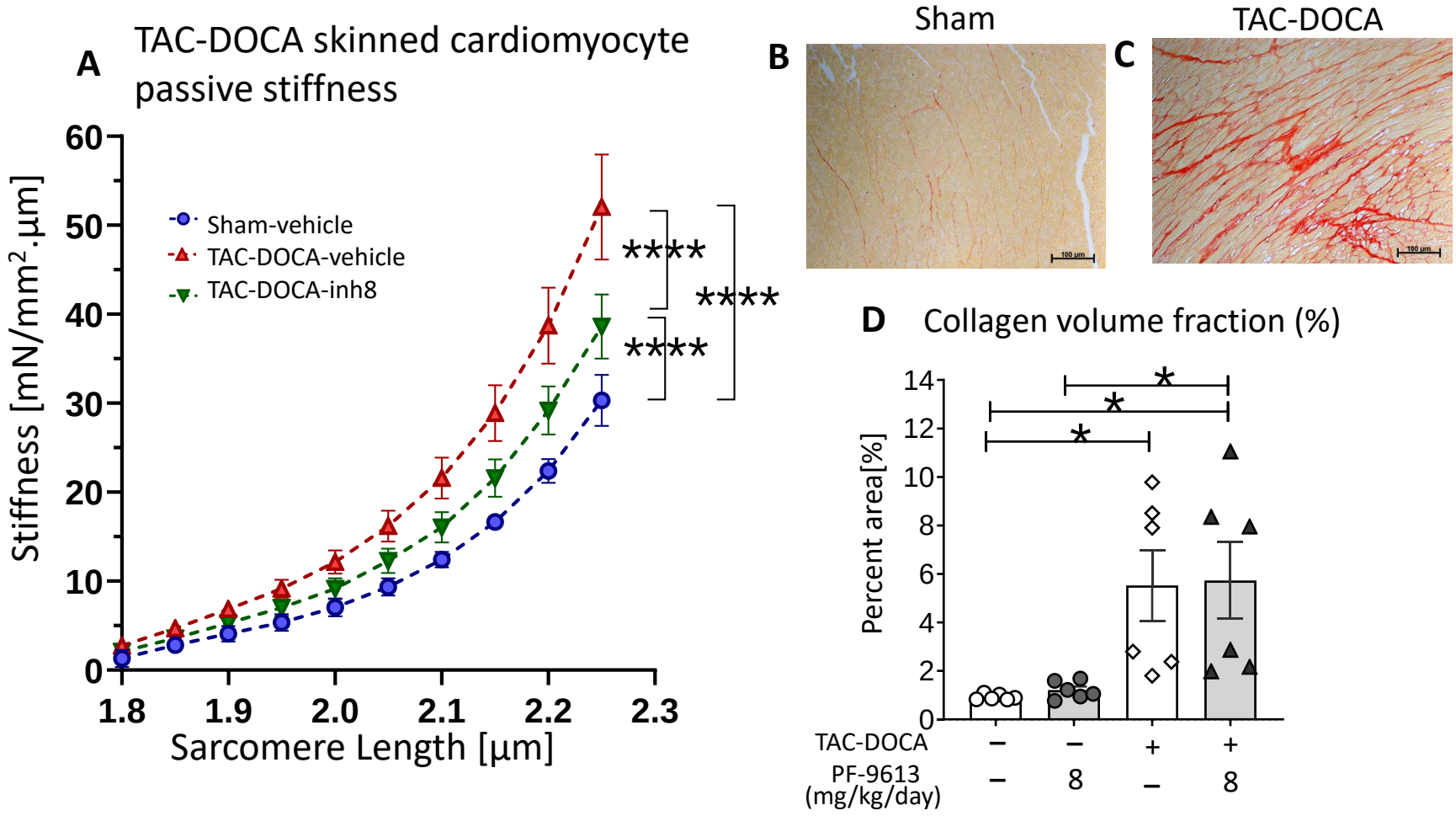

Figures 4. Cardiomyocyte passive stiffness, LV collagen content, LV *Pde9a* RNA expression, LV PDE9a activity, plasma cGMP and LV PKG activity of TAC-DOCA mice. Cardiomyocyte passive stiffness after chronic PDE9a inhibition, measured in demembraned (skinned) LV cardiomyocytes **(A)**. Cellular stiffness is increased in both groups of TAC-DOCA mice, however, the stiffness of TAC-DOCA-inh8 is lower than TAC-DOCA-veh (n= 7,15,14 cells from 4,8,7 mice) **(A)** . Representative Picrosirius Red staining for collagen of LV myocardium **(B &C)**. Quantitative analysis shows a significant increase in percent area of myocardial collagen in both groups of TAC-DOCA mice **(D).** No difference in percent area of collagen is observed between TAC-DOCA-veh and TAC-DOCA-inh8 (n=7, 6, 6 and 7 mice). Quantitative PCR was used to assess *Pde9a* RNA expression in LV myocardium. There is a significant upregulation of *Pde9a* mRNA at 5 weeks after TAC-DOCA surgery **(E)** (n=18,21 mice). High performance liquid chromatography was used to assess PDE9a activity in LV myocardium. PDE9a activity is increased in TAC-DOCA-veh but is normalized in TAC-DOCA-inh8 (n=7,7,6,9 mice) **(F)** . Plasma concentration of cGMP (**G)** and LV myocardial PKG activity (**H)** are increased in TAC-DOCA mice with PDE9a inhibition (n=10,9,12 mice for plasma cGMP and n=7,7,8 mice for PKG activity). * p≤0.05 ** p≤0.01 ***p≤0.001 ****p≤0.0001. Statistical analyses consisted of: (A) Nonlinear regression analysis with a least squares fitting, (D&F) two-way ANOVA without repeated measures with a Tukey test, (E) Mann-Whitney U test, (G) Kruskal-Wallis with a Dunn test, (H) One-way ANOVA without repeated measures with a Tukey test.

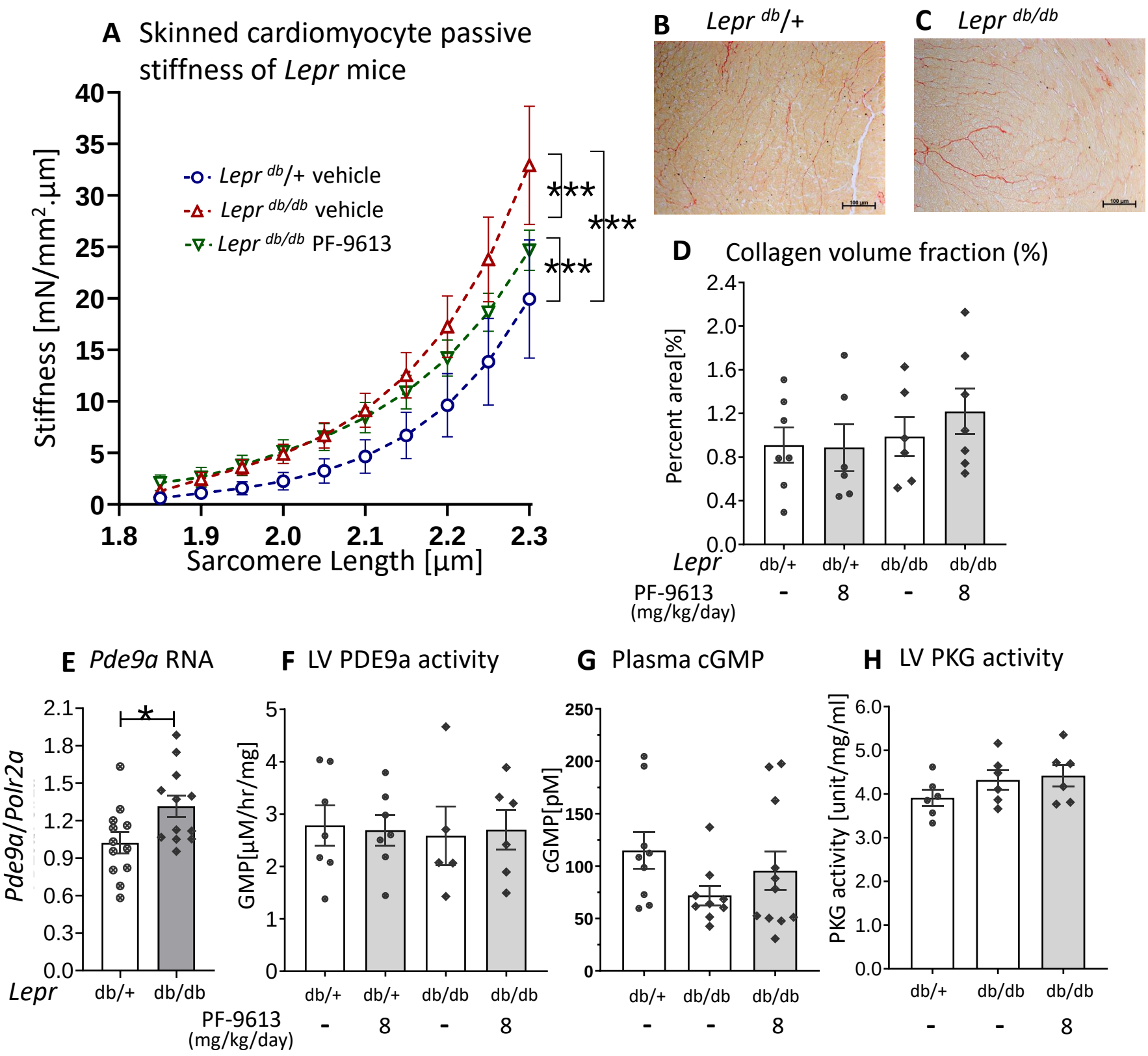

Figure 8. Cardiomyocyte passive stiffness, LV collagen content, LV *Pde9a* RNA expression, LV PDE9a activity, plasma cGMP and LV PKG activity of *Lepr$^{db/db}$* mice. Cardiomyocyte passive stiffness after chronic PDE9a inhibition, measured in demembraned (skinned) LV cardiomyocytes **(A)**. Cardiomyocyte stiffness is increased in both groups of *Lepr$^{db/db}$* mice, however the stiffness is slightly reduced in *Lepr$^{db/db}$* mice that were treated with PF-4449613 compared to vehicle **(A)** (n= 3,16,15 cells from 2,6,7 mice). Representative Picrosirius Red staining for collagen of LV myocardium **(B&C)**. Quantitative analysis does not show a significant difference in percent area of collagen among groups **(D)** (n=7, 6, 6 and 7 mice). There is a significant upregulation of *Pde9a* mRNA **(E)** (n=12,12 mice), however, there is no increase in PDE9a activity in LV myocardium of *Lepr$^{db/db}$* mice **(F)** (n= 7,7,5,6 mice). There is no increase in plasma cGMP concentration **(G)** or LV PKG activity **(H)** in *Lepr$^{db/db}$* mice with PDE9a inhibition (n =9,9,11 mice for plasma cGMP and n = 6,6,6 mice for LV PKG activity). * p≤0.05 ** p≤0.01 ***p≤0.001 ****p≤0.0001. Statistical analyses consisted of: (A) Nonlinear regression analysis with a least squares fitting, (D&F) Two-way ANOVA without repeated measures with a Tukey test (E) unpaired *t* test. (G) Kruskal-Wallis with a Dunn test. (H) One-way ANOVA without repeated measures with a Tukey test.

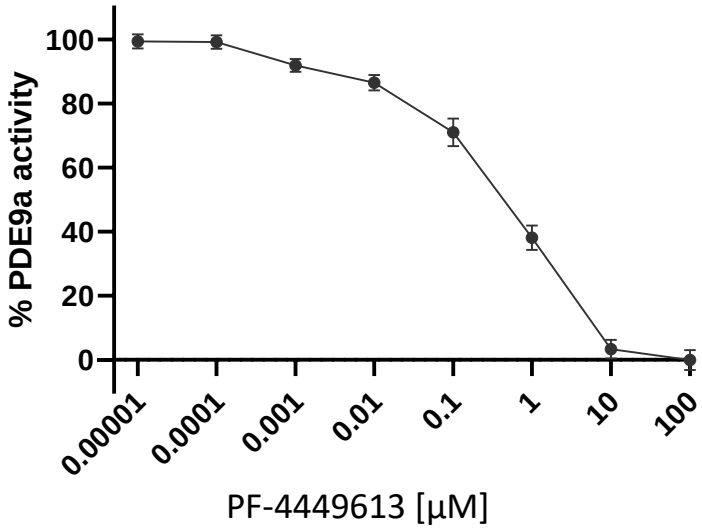

Supplemental Figure S1. Inhibition of PDE9a activity by PF-04449613. Inhibition of PDE9a activity by PF-4449613 is demonstrated. PF-4449613 is an effective inhibitor of PDE9a with an IC50 of 0.42 µM at substrate (cGMP) concentration of 200 nM and purified PED9a protein 8 pg/µL. Data performed in sextuplicate for each concentration.